IFIH1 (MDA5) is required for innate immune detection of intron-containing RNA expressed from the HIV-1 provirus

Mehmet Hakan Guney[a,1] (ID), Karthika Nagalekshmi[a,1] (ID), Sean Matthew McCauley[a] (ID), Claudia Carbone[a], Ozkan Aydemir[a] (ID), and Jeremy Luban[a,b,c,d,e,2] (ID)

Intron-containing RNA expressed from the HIV-1 provirus activates type 1 interferon in primary human blood cells, including CD4+ T cells, macrophages, and dendritic cells. To identify the innate immune receptor required for detection of intron-containing RNA expressed from the HIV-1 provirus, a loss-of-function screen was performed with short hairpin RNA-expressing lentivectors targeting twenty-one candidate genes in human monocyte-derived dendritic cells. Among the candidate genes tested, only knockdown of XPO1 (CRM1), IFIH1 (MDA5), or MAVS prevented activation of the interferon-stimulated gene ISG15. The importance of IFIH1 protein was demonstrated by rescue of the knockdown with nontargetable IFIH1 coding sequence. Inhibition of HIV-1-induced ISG15 by the IFIH1-specific Nipah virus V protein, and by IFIH1-transdominant 2-CARD domain-deletion or phosphomimetic point mutations, indicates that IFIH1 (MDA5) filament formation, dephosphorylation, and association with MAVS are all required for innate immune activation in response to HIV-1 transduction. Since both IFIH1 (MDA5) and DDX58 (RIG-I) signal via MAVS, the specificity of HIV-1 RNA detection by IFIH1 was demonstrated by the fact that DDX58 knockdown had no effect on activation. RNA-Seq showed that IFIH1 knockdown in dendritic cells globally disrupted the induction of IFN-stimulated genes by HIV-1. Finally, specific enrichment of unspliced HIV-1 RNA by IFIH1 (MDA5), over two orders of magnitude, was revealed by formaldehyde cross-linking immunoprecipitation (f-CLIP). These results demonstrate that IFIH1 is the innate immune receptor for intron-containing RNA from the HIV-1 provirus and that IFIH1 potentially contributes to chronic inflammation in people living with HIV-1, even in the presence of effective antiretroviral therapy.

HIV-1 | MDA5 | dendritic cells | type 1 interferon | unspliced RNA

Antiretroviral therapy (ART) suppresses HIV-1 viremia, protects CD4+ T cells, and prevents progression to AIDS, but it does not eliminate HIV-1 infection (1, 2). T cell activation markers that are elevated by HIV-1 infection are decreased after ART (3, 4), though systemic inflammation with activation of monocytes and macrophages remains an ongoing problem for many people living with HIV-1 on ART (5–8). Chronic immune activation is associated with non-AIDS-related complications of HIV-1 infection including elevated risk of cardiovascular disorders (9–12). In people living with HIV-1, Janus kinase inhibitor ruxolitinib decreased markers of inflammation (13), and pitavastatin reduced the risk of major adverse cardiovascular events (14). Given that inflammation is also a feature of aging, the magnitude of this public health problem is compounded by the increasing number of people living with HIV-1 who are over 50 y of age (15). Hence, better understanding of the chronic inflammation associated with HIV-1 infection would potentially aid clinical care of individuals with this chronic disease, as well as the public health response to it.

Several mechanisms have been proposed to contribute to chronic immune activation in people living with HIV-1 on ART. Some inhibitors of HIV-1 protease and integrase are associated with increased rates of obesity, metabolic syndrome, and other conditions linked to inflammation (16–18). The prevalence of infection with chronic pathogens, including herpes viruses, hepatitis viruses, and tuberculosis, is higher in people living with HIV-1, and these coinfections are associated with increased immune activation and cardiovascular disease risk (19–22). Destruction of CD4+ T$_H$17 cells during acute HIV-1 infection may weaken gut barrier function, permitting translocation of inflammatory microbial products from the intestinal lumen into the systemic circulation (23, 24). Similarly, homeostatic innate lymphoid cells within the gut lamina propria are permanently depleted by the cytokine storm that accompanies acute HIV-1 infection, contributing to disruption of gut barrier function (25, 26).

HIV-1 RNA expressed from proviruses is another factor that may contribute to chronic immune activation and inflammation in people living with HIV-1 on ART. Though ART

Significance

Antiretroviral therapy (ART) suppresses HIV-1 viremia and prevents progression to AIDS. Nonetheless, chronic inflammation is a common problem for people living with HIV-1 on ART. One possible cause of inflammation is ongoing transcription from HIV-1 proviruses, whether or not the sequences are competent for replication. Unspliced RNA produced by the HIV-1 provirus activates a type 1 interferon response, but the innate immune receptor that detects unspliced HIV-1 RNA is unknown. Here, in a targeted loss-of-function screen in primary human dendritic cells, we identified MDA5 as the innate immune receptor that detects HIV-1 RNA. These results suggest that MDA5 detection of unspliced HIV-1 RNA contributes to inflammation in people living with HIV-1, even in the presence of effective ART.

[1]M.H.G. and K.N. contributed equally to this work.

[2]To whom correspondence may be addressed. Email: jeremy.luban@umassmed.edu.

potently suppresses HIV-1 replication, it does not eliminate proviruses established prior to initiation of ART. In people living with HIV-1 on ART, such proviruses may persist in memory CD4+ T cells for the lifetime of the individual (1, 2, 27, 28), and possibly in other long-lived cell types such as liver macrophages (29–34). Over 95% of proviruses in people living with HIV-1 on ART have mutations which preclude production of infectious virus (35–37). Nonetheless, as much as 20% of these provirus-bearing cells express HIV-1 RNA (38–40). The amount of cell-associated HIV-1 RNA, rather than the quantity of intact HIV-1 provirus, correlates with T cell activation and plasma levels of inflammatory markers (41, 42). Collectively, these observations suggest that HIV-1 RNA promotes innate immune activation without requirement for new rounds of infection.

How the innate immune system detects HIV-1 RNA remains unclear, but mechanisms may differ depending on the target cell type and whether the infection is acute or chronic. HIV-1 RNA is detected by TLR7 during acute challenge of plasmacytoid dendritic cells (43–45), and possibly CD4+ T cells (46), but myeloid dendritic cells have limited expression of TLR7 and do not detect HIV-1 in the same manner (47–49). Transfection of HIV-1 genomic RNA activated RIG-I-dependent signaling (50, 51) but the relevance of RIG-I in the context of HIV-1 infection has not been confirmed. Detection of nascent HIV-1 cDNA by cyclic GMP-AMP synthase (cGAS) has been reported (52–55), while other research groups have failed to confirm the importance of cGAS for detection of HIV-1 (56–60). Such discrepancies might be explained by differences in protocol, including how HIV-1 challenge stocks are produced, the identity of the target cells, or CA amino acid residues that influence CA lattice stability (61–64).

We and others have reported that induction of innate immune signaling after HIV-1 challenge of primary human dendritic cells, macrophages, or CD4+ T cells requires integration, transcription from the nascent provirus, and nuclear export of intron-containing HIV-1 RNA through the Rev-CRM1 pathway (58, 59). The experiments described here had the goal of identifying the innate immune sensor of unspliced RNA produced by the HIV-1 provirus.

Results

Loss-of-Function Screen in Dendritic Cells for Genes Required for Detection of Intron-Containing RNA Expressed from the HIV-1 Provirus.
HIV-1 transduction activates innate immune signaling and type 1 IFN in human blood CD4+ T cells, monocyte-derived dendritic cells, and monocyte-derived macrophages (52, 54, 55, 58, 59, 65). This host response requires HIV-1 reverse transcription, integration, transcription from the provirus, and expression of the CRM1-dependent, Rev-dependent, Rev Response Element (RRE)-containing, unspliced HIV-1 RNA (58, 59). To identify host genes required for innate immune detection of unspliced RNA expressed from the HIV-1 provirus, a targeted loss-of-function screen was performed in which twenty-one host genes encoding previously described HIV-1 RNA binding proteins (66–68), or well-characterized innate immune nucleic acid receptors, were knocked down in dendritic cells, and ISG15-induction by HIV-1 transduction was monitored by flow cytometry (58).

As previously described (58, 69), human CD14+ monocytes were enriched from peripheral blood mononuclear cells (PBMCs) with magnetic beads and transduced with lentivectors encoding puromycin acetyltransferase and a short hairpin RNA (shRNA) designed to knockdown transcripts from one of the candidate genes (Fig. 1A). To increase transduction efficiency, monocytes were challenged simultaneously with virus-like particles (VLPs) bearing simian immunodeficiency virus (SIV)$_{MAC}$251 Vpx (70).

For the primary screen, each candidate gene was targeted by three different shRNAs, using monocytes from two blood donors. An shRNA that targets luciferase (Luc) was used as a negative control. Immediately following incubation with Vpx+ VLPs and the knockdown vector, monocytes were placed in culture with IL-4 and GM-CSF produced in human cells to promote differentiation into dendritic cells. Three days after transduction, puromycin was added to the medium to select for cells that had been transduced. The dendritic cells that result from this protocol are immature and do not express interferon-stimulated genes (Fig. 1B and refs. 58, 59, and 65).

On day seven, the resulting immature dendritic cells were challenged with single-cycle HIV-1 produced by transfection of HIV-1 proviral DNA bearing a deletion in *env* and enhanced green fluorescent protein (GFP) in place of *nef* (HIV-1-GFP), along with a vesicular stomatitis virus glycoprotein (VSV G) expression plasmid (71) (Fig. 1A). VSV G pseudotyping increases transduction efficiency, though dendritic cells mature in response to transduction using the HIV-1 glycoprotein and in the absence of Vpx+ VLPs (58). Dendritic cells were then assessed by flow cytometry for GFP and ISG15 protein levels (Fig. 1B). ISG15 was evident in both HIV-1-GFP-transduced and -untransduced dendritic cells (58), an observation explained previously as bystander activation by secreted IFN-β (65). Additionally, Vpx+ VLPs alone had no effect on ISG15 levels.

Of the 21 candidate genes targeted in our screen, only knockdown of XPO1 (Exportin 1, also called CRM1), IFIH1 (also known as MDA5), or MAVS, inhibited ISG15 induction in response to HIV-1-GFP (Fig. 1C). Reduction in ISG15 signal by XPO1 knockdown is expected since XPO1-inhibitors blocked ISG15 induction in dendritic cells in response to HIV-1 transduction (58, 59). Given that IFIH1 detects viral dsRNA (72, 73) and activates type 1 IFN via interaction with MAVS, IFIH1 seemed a plausible candidate for the innate immune receptor that detects unspliced HIV-1 RNA. Therefore, subsequent experiments focused on IFIH1 and MAVS. Knockdown of DDX58 (also known as RIG-I), an innate immune receptor that also signals via MAVS, had no effect on ISG15-induction by HIV-1 (Fig. 1C).

To validate the results of the primary screen, the importance of IFIH1 and MAVS for innate immune detection of HIV-1 was tested using dendritic cells from four additional blood donors. DDX58 was targeted as a negative control. Western blot of cell lysates from dendritic cells transduced with lentiviral vectors expressing three separate shRNAs for each gene reduced protein levels for MAVS by 6-, 4.5-, and 6-fold, for DDX58 by 10-, 14-, and 42-fold, and for IFIH1 by 8-, 22-, and 26-fold, respectively (Fig. 2A). Again, knockdown of MAVS or IFIH1 blocked the ISG15 induction that resulted from HIV-1 transduction (Fig. 2B). In contrast, DDX58 knockdown had no effect on ISG15 induction (Fig. 2B). Decreased ISG15 induction might result if shRNAs targeting MAVS or IFIH1 decreased the efficiency of subsequent HIV-1 transduction, but none of the shRNAs targeting these genes decreased HIV-1 infectivity (Fig. 2C).

IFIH1 and MAVS Are Required to Sense HIV-1 RNA in Monocyte-Derived Macrophages.
The importance of IFIH1 and MAVS for innate immune detection of HIV-1 in monocyte-derived macrophages was examined next. Macrophages were generated from CD14+ blood monocytes by culturing for 7 d in the presence of GM-CSF, as previously described (58, 69). Cells were incubated with Vpx+ VLPs and transduced with lentivectors expressing shRNAs specific for IFIH1 and MAVS, and selected with puromycin, as described above for DCs. Cells were then challenged with HIV-1-GFP. As with the dendritic cells, ISG15 induction was blocked when either IFIH1 or MAVS was knocked
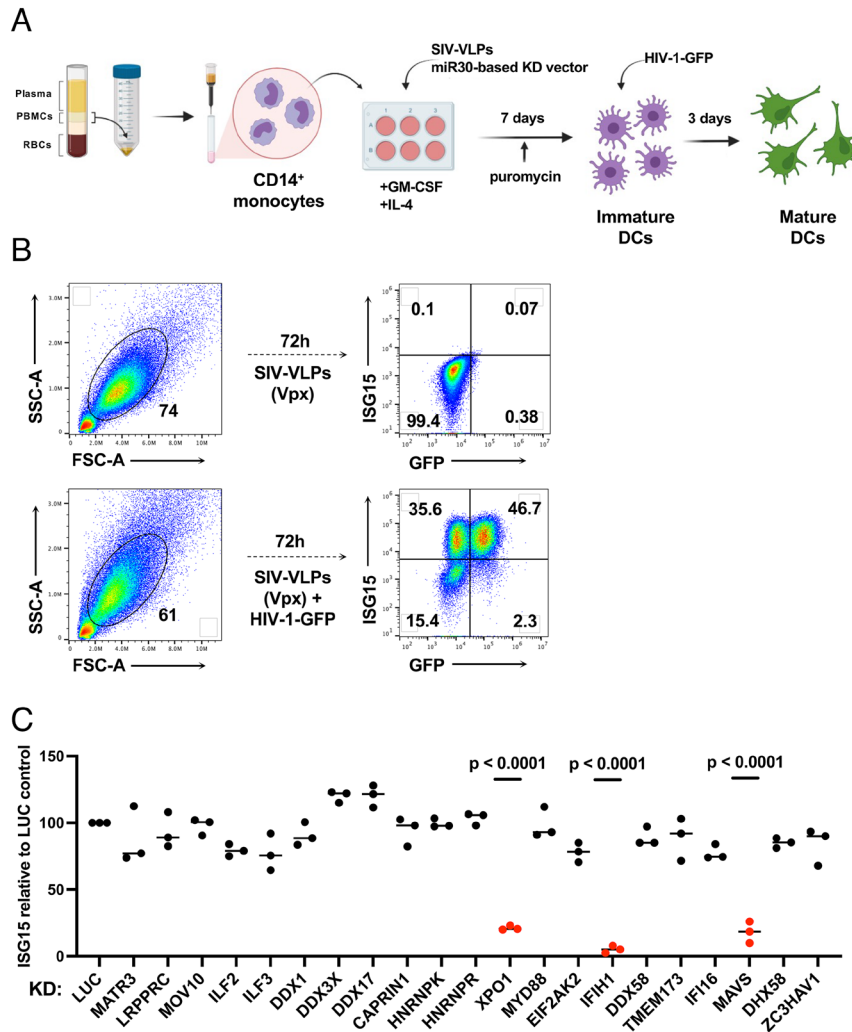
Fig. 1. Targeted loss-of-function screen in dendritic cells identified IFIH1, MAVS, and XPO1 as required for ISG15-induction by HIV-1 transduction. (*A*) Schematic showing the experimental design of the knockdown screen in monocyte-derived dendritic cells. CD14⁺ monocytes transduced with shRNA-puromycin resistance vectors were differentiated into dendritic cells and selected with puromycin. Differentiated cells were transduced with HIV-1-GFP on day 7. Three days later, cells were stained for intracellular ISG15 and analyzed by flow cytometry. (*B*) Representative gating strategy for flow cytometry data presented in this manuscript. (*C*) Loss-of-function screen in dendritic cells targeting 21 genes encoding HIV-1 RNA binding proteins or innate immune receptors. The plot depicts ISG15 signal upon HIV-1-GFP transduction after suppressing the indicated candidate gene relative to ISG15 signal in Luciferase control knockdown cells (n = 3 shRNA target sites, n = 2 donors). *P* values were determined by one-way ANOVA with Dunnett's multiple comparisons test, relative to luciferase knockdown control.

down (Fig. 3*A*), and knockdown of IFIH1 or MAVS with shRNA lentivectors did not affect the efficiency of subsequent transduction by HIV-1 (Fig. 3*B*).

The role of IFIH1 and DDX58 in innate immune signaling has previously been established in the context of RNA viruses other than HIV-1. More specifically, type 1 IFN induction by encephalomyocarditis virus (EMCV) is IFIH1-dependent (74), but induction by Sendai virus (SeV) is IFIH1-independent (75, 76). Challenges with these two viruses were used to determine whether the behavior of the shRNA-knockdown macrophages is consistent with this literature. Indeed, EMCV and SeV each independently induced ISG15 protein production in the macrophages (Fig. 3*C*), and IFIH1 knockdown prevented ISG15-induction by EMCV but not by SeV (Fig. 3*C*). Overall, these data suggest that IFIH1 and MAVS play a critical role in innate immune sensing of nascent RNA produced by the HIV-1 provirus within human myeloid cells.

Human IFIH1 Protein Is Required for Innate Immune Sensing of HIV-1 RNA in Myeloid Cells. To rule out potential off-target effects of IFIH1 shRNAs, and to test whether IFIH1 protein

is sufficient for innate immune detection of HIV-1 RNA, a previously described all-in-one knockdown and target protein rescue vector (69) was used to simultaneously express both the shRNA that targets endogenous IFIH1 RNA, and human IFIH1 coding sequence containing silent mutations in the shRNA target sequence, from a single primary transcript. Four versions of the all-in-one vector were engineered, each containing a different combination of shRNAs, targeting either IFIH1 or Luc control, and open reading frames (ORF), encoding either nontargetable IFIH1 or heat stable antigen (HSA)/CD24 as a control ORF (Fig. 4*A*).

Dendritic cells and macrophages were transduced with each of the four versions of the all-in-one vector and selected for 3 d with puromycin. Cells were then challenged with the HIV-1-GFP reporter vector, and 3 d later assessed by western blot for steady-state levels of IFIH1 protein (Fig. 4*B*), and by flow cytometry for the percentage of ISG15⁺ cells (Fig. 4 *C* and *D*). In both dendritic cells and macrophages, transduction with the vector expressing the IFIH1-specific shRNA and the HSA coding sequence reduced IFIH1 protein levels (Fig. 4*B*) and abrogated ISG15-induction by HIV-1 (Fig. 4 *C* and *D*). Transduction with
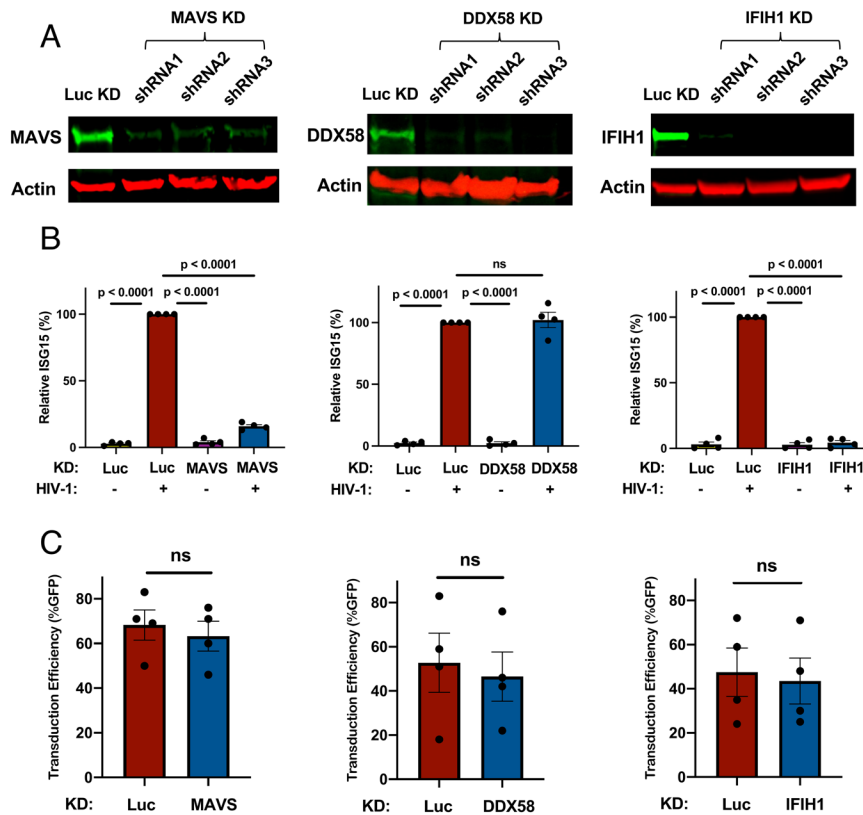
Fig. 2. Knockdown of IFIH1 or MAVS in dendritic cells prevents ISG15-induction by HIV-1. (*A*) CD14^{+} monocytes were transduced with shRNA-puromycin resistance vectors targeting MAVS, DDX58, IFIH1, or luciferase (Luc) control, as indicated, and cells were differentiated into dendritic cells under puromycin selection as in Fig. 1*A*. Representative immunoblots show the protein signal in the indicated samples. (*B*) Differentiated cells were transduced with HIV-1-GFP for 3 d, and then assessed by flow cytometry for intracellular ISG15. Plots show relative ISG15 signal in the indicated knockdown cells, with and without HIV-1-GFP transduction (mean ± SEM, n = 4 donors). *P* values were determined by one-way ANOVA with Tukey's multiple comparisons test. (*C*) Percentage GFP^{+} cells after HIV-1-GFP transduction of the dendritic cells in *B* (mean ± SEM, n = 4 donors). *P* values were determined by the two-tailed, paired *t* test.

the vector expressing the IFIH1-specific shRNA and the nontargetable IFIH1 coding sequence restored IFIH1 protein to the level in control cells (Fig. 4*B*) and the induction of ISG15 by HIV-1 to the control level (Fig. 4 *C* and *D*). Finally, cells transduced with vector bearing shRNA targeting Luc and HSA coding sequence behaved like control cells (Fig. 4 *B–D*). These results demonstrate that IFIH1 protein is required for innate immune sensing of HIV-1 RNA in both human dendritic cells and macrophages and that disruption of this activity by the shRNA was not due to off-target effects of the transduction vectors or the shRNAs.

Filament Formation by IFIH1 Is Required for Innate Immune Detection of HIV-1. As an orthogonal method to test the specific requirement for IFIH1 in innate sensing of HIV-1, CD14^{+} monocytes were transduced with a vector engineered to express Nipah virus V protein and puromycin acetyltransferase, or with a control vector lacking the Nipah virus V coding sequence. Paramyxovirus V proteins bind to the SF2 ATP hydrolysis domain of IFIH1, but not of DDX58, and prevent the formation of filaments that is required for activation of MAVS (77–81). Transfected cells were selected with puromycin and differentiated into dendritic cells and macrophages. These puromycin-selected myeloid cell populations were then challenged with HIV-1-GFP and 3 d later the percentage of ISG15^{+} cells was assessed by flow cytometry.

Transduction and selection with the Nipah virus V protein-expression vector blocked ISG15-induction by HIV-1 in either dendritic cells or macrophages (Fig. 5 *A* and *B*). Since IFIH1 is required for innate immune detection of EMCV (74) this virus was used as a positive control; as expected, prior transduction with

the Nipah virus V-expression vector also decreased ISG15-induced by EMCV (Fig. 5*C*). In contrast, Nipah virus V had no effect on ISG15-induction by SeV (Fig. 5*D*), consistent with the fact that this virus is detected by DDX58, an innate sensor that is not blocked by V protein (75, 76). Given the previously demonstrated biochemical effects of paramyxovirus V proteins (77–81), these experiments indicate that dsRNA-stimulated filament formation by IFIH1 is required for innate immune detection of HIV-1.

IFIH1 Dephosphorylation and Association with MAVS Is Required for ISG15 Activation by HIV-1. Innate immune signaling by IFIH1 requires interaction of its N-terminal tandem caspase activation and recruitment domains (CARDs) with MAVS (72, 73, 82, 83). Furthermore, phosphorylation of IFIH1 serine 88 inhibits interaction with MAVS, and phosphomimetic mutations at this position are resistant to activation (84). Given that IFIH1 binds RNA as a dimer, which cooperatively forms filaments on long dsRNAs (85–87), IFIH1 with critical loss-of-function mutations would be expected to disrupt endogenous IFIH1 activity in trans. To test whether type 1 IFN induction by HIV-1 requires that IFIH1 signal via MAVS, an IFIH1 CARD-deletion mutant (IFIH1-2CARD), and two phosphomimetic mutants, IFIH1-S88D and -S88E, were engineered into puromycin-selectable, lentiviral expression plasmids (Fig. 6*A*). When monocytes were transduced with a lentivector encoding WT IFIH1, or with any of the 3 IFIH1 mutants, ISG15 induction in the resulting dendritic cells was not detected in the absence of HIV-1 challenge, indicating that transduction with the IFIH1 expression vectors alone did not activate type 1 IFN (Fig. 6*B*). When dendritic cells were challenged with HIV-1, ISG15 induction was detected as
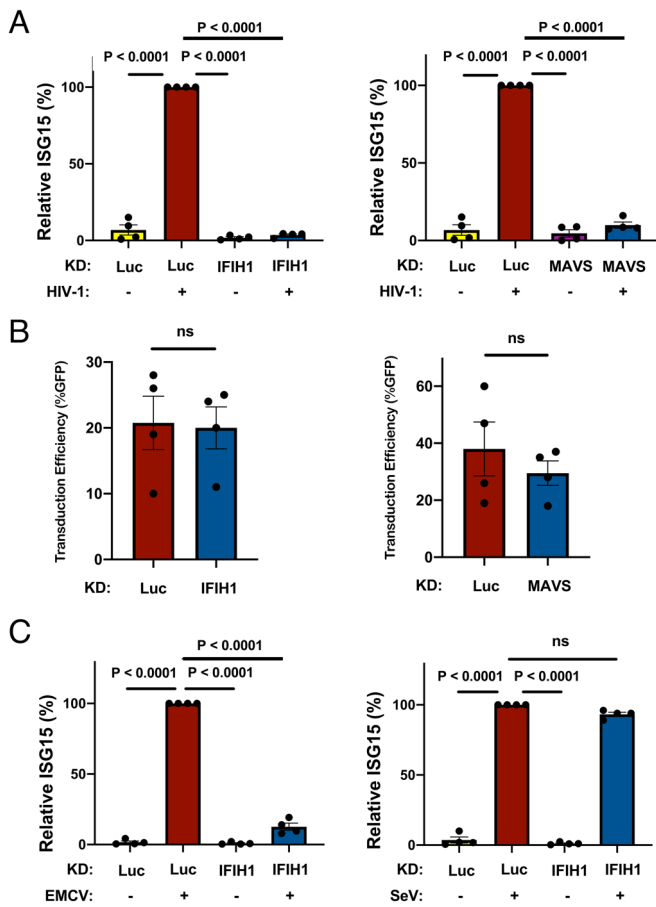
Fig. 3. IFIH1 or MAVS knockdown prevents ISG15-induction by HIV-1 in macrophages. (*A*) CD14+ monocytes were transduced with shRNA-puromycin resistant vectors targeting IFIH1, MAVS, or LUC control, as indicated. Cells were selected with puromycin for 3 d, and differentiated into macrophages in the presence of GM-CSF. Cells were transduced with HIV-1-GFP for 3 d and then assessed by flow cytometry for intracellular ISG15. Plots show relative ISG15 signal in the indicated knockdown cells, with and without HIV-1-GFP transduction (mean ± SEM, n = 4 donors). *P* values were determined by one-way ANOVA with Tukey's multiple comparisons test. (*B*) Quantification of GFP+ cell populations in donors used in the experiments for *A* (mean ± SEM, n = 4 donors). *P* values were determined by the two-tailed, paired *t* test. (*C*) As in *A*, except that macrophages were infected with either encephalomyocarditis virus (EMCV) or Sendai virus (SeV), instead of with HIV-1-GFP (mean ± SEM, n = 4 donors). *P* values were determined by one-way ANOVA with Tukey's multiple comparisons test.

Fig. 4. IFIH1 (MDA5) protein is required for ISG15-induction by HIV-1 in myeloid cells. (*A*) Schematic representation of all-in-one shRNA-rescue lentivector, in which the SFFV promoter expresses a tripartite fusion of puromycin N-acetyltransferase (puroR), the K48R mutant of ubiquitin (UbK48R), and an ORF encoding the gene of interest, as well as a modified miR30-based shRNA (miR-30). (*B–D*) All-in-one lentivectors encoding HSA/CD24, or nontargetable, shRNA-resistant IFIH1 coding sequence (ntIFIH1), along with shRNA targeting Luc or IFIH1 as indicated in *A*, were used to transduce dendritic cells (*B* and *C*), or macrophages (*D*). (*B*) Representative immunoblot for quantification of IFIH1 (MDA5) protein levels in indicated samples. (*C* and *D*) The percentage of ISG15+ cells was quantified by flow cytometry 3 d after HIV-1-GFP transduction and normalized to 100% for HSA ORF/Luc-knockdown cells (mean ± SEM, n = 4 donors for each). *P* values were determined by one-way ANOVA with Tukey's multiple comparisons test.

was reduced 27-, 62-, and 72-fold, respectively (Fig. 7*A*). The transduced dendritic cells were then challenged with HIV-1-GFP or left untreated. Forty-eight hours later, RNA was isolated from these cells and used to generate poly(A)-selected RNA-Seq libraries.

As compared to uninfected cells, HIV-1 transduction of control Luc knockdown cells increased expression of 464 genes and decreased expression of 106 genes (Fig. 7*B* and *SI Appendix,* Table S1, cutoff log$_2$ ≥1 and *P* value ≤ 0.05). Among the up-regulated interferon-stimulated genes, APOBEC3A, CXCL10, and ZBP1 were all increased well over 1,000-fold (*P* < 0.0001), DDX58 was increased 23-fold (*P* < 0.0001), and IFIH1 was increased 11-fold (*P* < 0.0001). In contrast, the number of differentially expressed genes was greatly decreased after HIV-1 challenge of IFIH1 knockdown cells, with 53 genes increased and 5 genes decreased (Fig. 7*C* and *SI Appendix,* Table S2, cutoff log$_2$ ≥1 and *P* value ≤ 0.05). Reactome pathway analysis of these differentially expressed genes showed enrichment for type 1 IFN signaling, interferon genes, and regulators of IFIH1/RIG-I signaling (Fig. 7*D*). Transcriptional profiling demonstrated that HIV-1 transduction of dendritic cells activates a large collection of interferon-stimulated genes and that IFIH1 is largely required for this induction.

Unspliced HIV-1 RNA in Dendritic Cells Associates Specifically with IFIH1. To determine whether unspliced HIV-1 RNA expressed from proviruses in dendritic cells binds specifically to IFIH1, cells transduced with HIV-1-GFP were subjected to formaldehyde cross-linking immunoprecipitation (f-CLIP) (88). Protein A-coated magnetic beads were incubated with affinity-purified, polyclonal rabbit anti-IFIH1 IgG, or with the equivalent anti-DDX58 IgG as a control. Beads with the bound IgG were then used to immunoprecipitate protein from formaldehyde-cross-linked dendritic cell lysates. Western blot showed that recovery of IFIH1 and DDX58 proteins was specific and quantitative, with no residual protein detected in the unbound fraction (Fig. 8*A*). cDNA was generated from the RNA that remained bound to the

expected in those cells that had been transduced with WT IFIH1 (Fig. 6*B*). In contrast, as compared to dendritic cells transduced with WT IFIH1, ISG15 induction after HIV-1 challenge was reduced 10.4-fold, 17.5-fold, and 8.9-fold in the dendritic cells that had been transduced with the IFIH1-2CARD, -S88D, or -S88E mutants, respectively (Fig. 6*B*). Prior transduction with lentiviral vectors expressing WT IFIH1 or any of the three IFIH1 mutants did not change the efficiency of subsequent transduction by HIV-1 (Fig. 6*C*). These data demonstrate that IFIH1-dependent detection of HIV-1 requires signaling through the canonical MAVS pathway.

Effect of HIV-1 Transduction and IFIH1 Knockdown on the Dendritic Cell Transcriptome. The effect of HIV-1 transduction and of IFIH1 knockdown on changes to the dendritic cell transcriptome was examined next using RNA-Seq. CD14+ monocytes from three blood donors were each transduced with lentivectors encoding shRNAs specific for either IFIH1 or control Luc. Transduced cells were selected with puromycin and differentiated into dendritic cells. Western blot showed that, in cells expressing the IFIH1-specific shRNA from donors M27, M28, and M29, IFIH1 protein
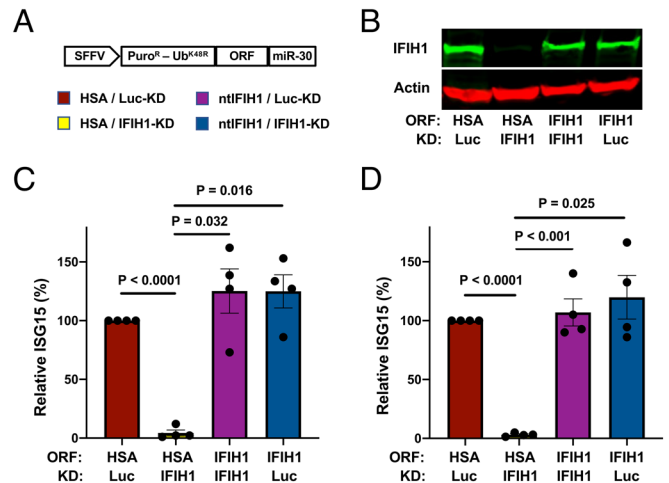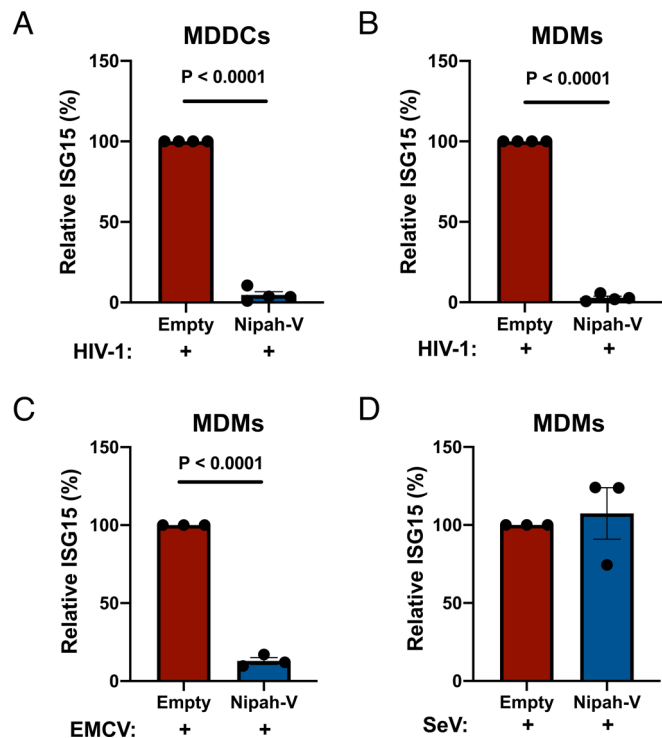
Fig. 5. Nipah virus V protein prevents ISG15-induction by HIV-1. (*A* and *B*) Nipah virus V protein was expressed from a lentivector in dendritic cells (*A*), or macrophages (*B*), and cells were subsequently transduced with HIV-1-GFP for 3 d. The percentage of ISG15$^+$ cells was quantified by flow cytometry and normalized to the values for cells expressing the empty vector (mean ± SEM, n = 4 donors for each). *P* values were determined by the two-tailed, paired *t* test. (*C* and *D*) Nipah virus V protein was expressed in macrophages and subsequently either infected with EMCV (*C*) or SeV (*D*). The percentage of ISG15$^+$ cells was measured by flow cytometry and normalized to the values for cells expressing the empty vector (mean ± SEM, n = 3 donors for each). *P* values were determined by the two-tailed, paired *t* test.

beads after extensive washing, and the cDNA was then amplified by qPCR using primers specific for HIV-1 (Fig. 8*B*). qPCR cycle threshold values (Ct) were used to calculate the fold enrichment of HIV-1 RNA relative to the cellular gene ACTB. Unspliced HIV-1 RNA was amplified using oligonucleotide primers specific to *gag*, or to coding sequences for RT or IN (Fig. 8*B*), and was enriched on IFIH1, 352.5-fold, 226.8-fold, and 466.7-fold, respectively (Fig. 8*C* shows the average fold enrichment for three blood donors, all *P* < 0.0001). Spliced HIV-1 RNA was not enriched on IFIH1 (Fig. 8*C*), whether it retained the RRE (D1A4) or not (D4A7). None of the HIV-1 RNAs were enriched on DDX58 (Fig. 8*C*). These results demonstrate that there is specific interaction between IFIH1 and unspliced HIV-1 RNA in dendritic cells.

Discussion

Here, a targeted loss-of-function screen based on lentiviral delivery of shRNAs in dendritic cells identified IFIH1 and its downstream signaling molecule MAVS, as required for innate immune detection of intron-containing RNA expressed from the HIV-1 provirus (Fig. 1*C*). These findings with IFIH1 and MAVS were confirmed using cells from multiple blood donors (Fig. 2). Rescue of the knockdown with a nontargetable cDNA demonstrated the importance of IFIH1 protein for detection of HIV-1 (Fig. 4), and RNA-Seq showed that IFIH1 knockdown prevented induction of the majority of interferon-stimulated genes (Fig. 7). Inhibition of HIV-1-induced, interferon-stimulated genes, by the IFIH1-specific Nipah virus V protein (Fig. 5), and by IFIH1-transdominant inhibitory CARD-deletion or phosphomimetic point mutations (Fig. 6), are consistent
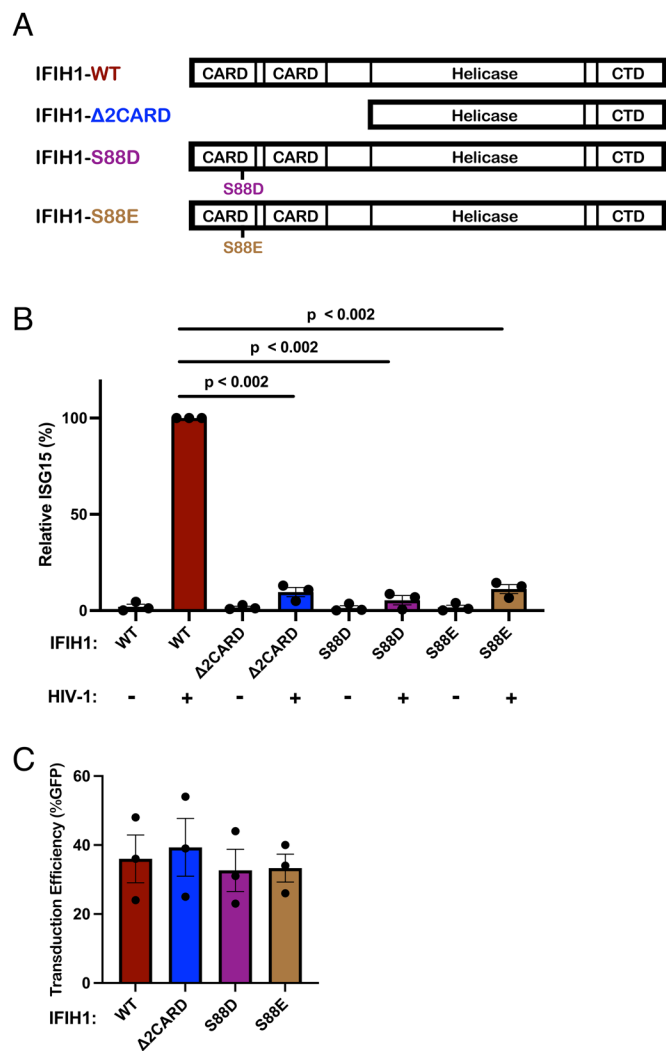

Fig. 6. IFIH1 mutants defective for interaction with MAVS act in trans to abrogate ISG15-induction by HIV-1 in dendritic cells. (*A*) Schematic of the IFIH1 domain structure and mutants generated here. (*B*) Dendritic cells were transduced with either the vector expressing human codon optimized WT IFIH1 or one of the three indicated IFIH1 mutants. After selection with puromycin, cells were transduced with HIV-1-GFP for 3 d. The percentage of ISG15$^+$ cells was quantified by flow cytometry and normalized to the values for cells expressing WT IFIH1 (mean ± SEM, n = 3 donors for each). *P* values were determined by one-way ANOVA with Dunnett's multiple comparisons test. (*C*) Quantification of GFP$^+$ cell populations in donors used in the experiments for *B*, mean ± SEM, n = 3 donors.

with the idea that IFIH1 filament formation and dephosphorylation, as well as association with MAVS, are required for innate immune activation in response to HIV-1 transduction. Finally, as compared with a control cellular RNA, unspliced HIV-1 was enriched several hundred-fold by IFIH1 protein, but not by DDX58 (Fig. 8). Spliced HIV-1 RNA was enriched by neither IFIH1 nor DDX58 (Fig. 8). These results show that interferon-stimulated gene activation by transcription from the HIV-1 provirus requires IFIH1 recognition of *rev*-dependent, CRM1-dependent, intron-containing RNA, and IFIH1 filament formation, dephosphorylation, and association with MAVS.

Though MAVS was required for innate immune detection of HIV-1 (Fig. 1), and both IFIH1 and DDX58 activate type 1 interferon via MAVS (89–92), the specificity of HIV-1 RNA recognition was demonstrated by failure of a 10 to 42-fold DDX58 protein reduction to block innate immune activation by HIV-1 (Figs. 1 and 2). That being said, despite the use of three individual shRNAs to knockdown each candidate gene, it is possible that the
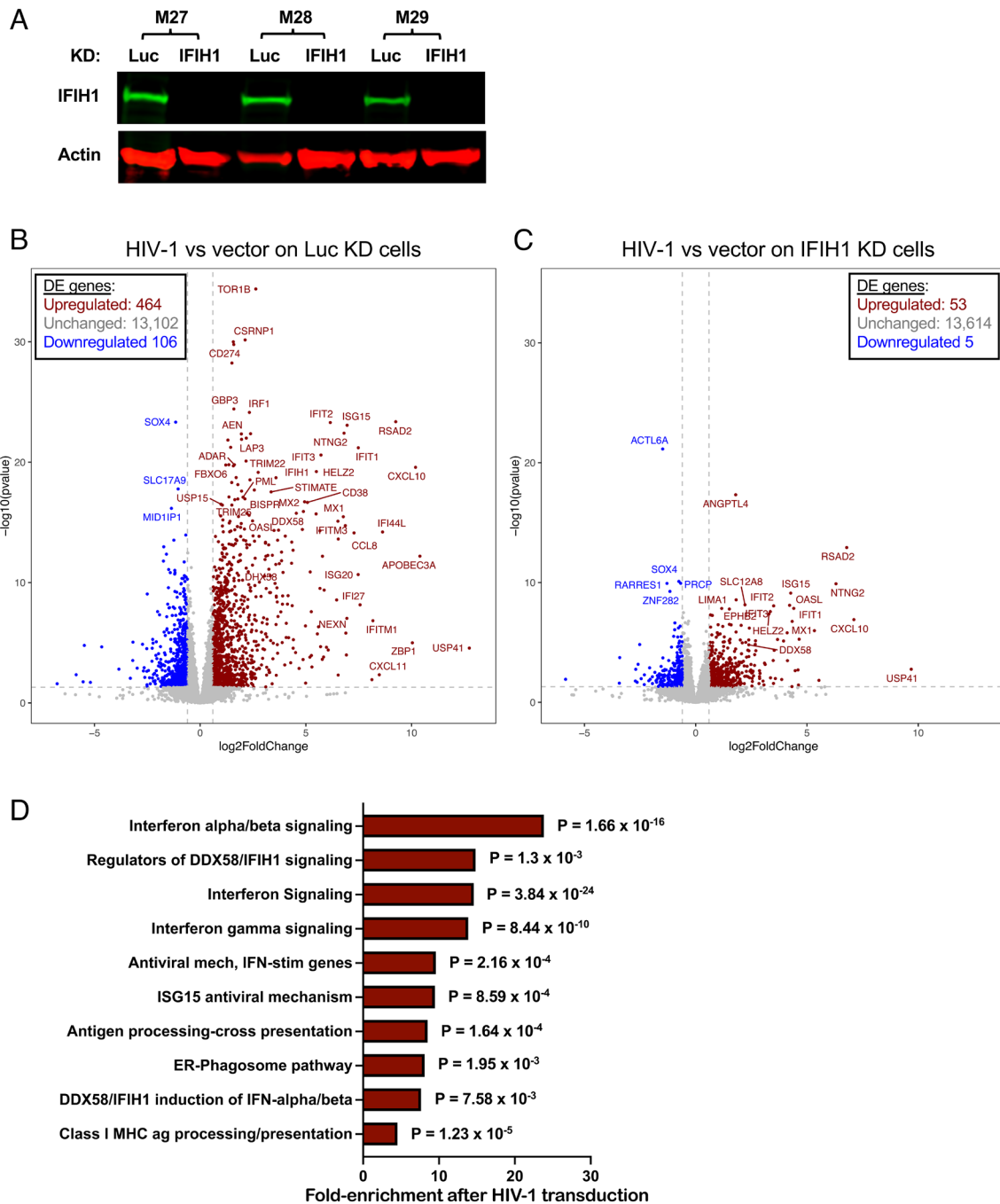
Fig. 7. Effect of HIV-1 transduction and of IFIH1 knockdown on the dendritic cell transcriptome. CD14^{+} monocytes from three blood donors (coded M27, M28, and M29) were transduced with shRNA-puromycin resistance vectors targeting either IFIH1 or Luc control, as indicated. Cells were selected with puromycin for 3 d, and differentiated into dendritic cells. (*A*) Immunoblot shows steady-state levels of IFIH1 (MDA5) protein for the indicated samples. Then, dendritic cells were either transduced with HIV-1-GFP or left untransduced. At 48 h, RNA was isolated from cells, and poly(A)-selected libraries were generated for RNA-Seq. Volcano plot depicting differentially expressed genes after HIV-1 challenge in Luc knockdown control cells (*B*), or in IFIH1-knockdown cells (*C*), as determined by DESeq2 combining RNA-Seq data from the three blood donors. Red dots indicate genes with log2 fold change of normalized counts >1; $P < 0.01$. Blue dots indicate the log2 fold change of normalized counts <−1; $P < 0.01$. Gray dots failed to achieve either criterion. (*D*) Reactome pathway analysis based on 276 differentially expressed genes in HIV-1 transduced Luc-knockdown cells in comparison to HIV-1 transduced IFIH1-knockdown cells. Gene Ontology-produced *P* values (as determined by Fisher's exact test) with FDR correction (Benjamini–Hochberg method) are shown. *SI Appendix*, Tables S1 and S2 show differentially expressed genes in *B* and *C*, respectively.

knockdown efficiency of DDX58, or of the other 17 genes that failed to score in our screen, was simply inadequate to result in a phenotype. This is an inherent weakness of loss-of-function experiments, exemplified by previous studies with LEDGF: Only after intensive knockdown of this chromatin-associated protein was an HIV-1 replication phenotype evident (93).

IFIH1 and DDX58 discriminate viral RNAs from cellular RNAs based on unique molecular features of the viral RNAs. DDX58, for example, binds to di- or triphosphate groups that are sometimes found

at the 5′-end of viral RNAs, but not on cellular RNAs (94–101). It therefore makes sense that HIV-1 RNA was not detected by DDX58 (Figs. 1, 2, and 8) since HIV-1 RNA lacks 5′-phosphates and instead possesses either a 7-methylguanosine or a hypermethylated cap (102, 103). Stable interaction with IFIH1, instead, has been shown to require double-stranded RNA 1,000 nucleotides in length, such as the double-stranded RNA intermediates generated during viral replication (83, 85, 104–106). HIV-1 RNA structural studies have identified highly structured regions with double-stranded character, but
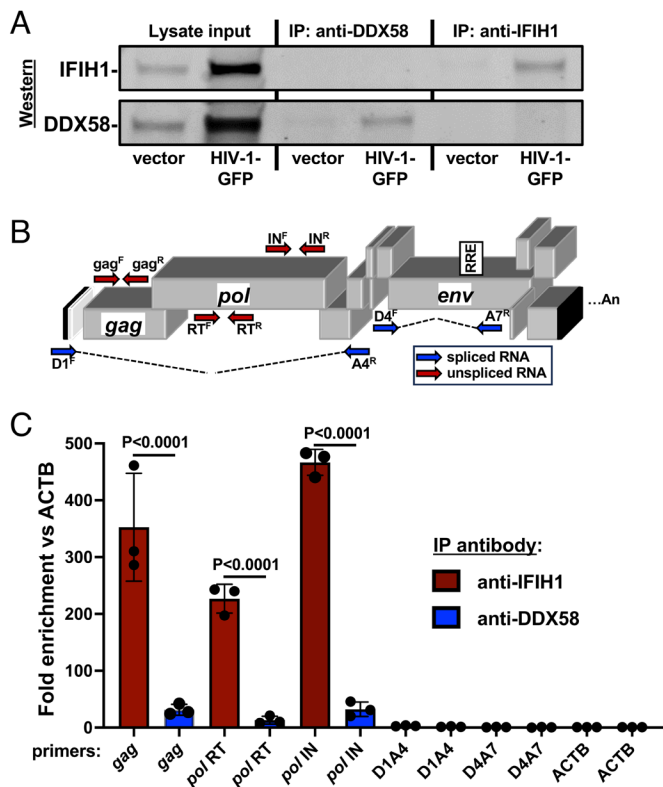
Fig. 8. Unspliced HIV-1 RNA expressed from the provirus in dendritic cells associates specifically with IFIH1. Dendritic cells generated from three blood donors were transduced with HIV-1 GFP, or with minimal HIV-1 vector. At 72 h, cells were cross-linked with formaldehyde and proteins were immunoprecipitated using affinity-purified rabbit IgG specific for IFIH1 (IP:anti-IFIH1) or DDX58 (IP: anti-DDX58), as indicated. (*A*) Western blot of cell lysate used for immunoprecipitation, anti-DDX58 immunoprecipitate, and anti-IFIH1 immunoprecipitate, probed using antibody targeting IFIH1 (*Upper* row) or DDX58 (*Lower* row). (*B*) Schematic of the HIV-1 genome showing the location of qPCR primers that detect unspliced (red) or spliced (blue) transcripts. (*C*) Fold enrichment of HIV-1 RNA in immunoprecipitates obtained with anti-IFIH1 antibody (red bars) or anti-DDX58 antibody (blue bars), as determined by RT-qPCR using primers specific for the RNAs indicated across the *X* axis. Each bar shows the mean value relative to ACTB for dendritic cells obtained from three individual blood donors, ±the SEM. *SI Appendix*, Table S4 shows the primers used in RT-qPCR here.

the longest stems are maximally 40 nucleotides in length (107, 108). Perhaps complex stem-loop structures bearing both double-stranded and single-stranded structures like those reported for the 5'UTR and the RRE are sufficient for IFIH1 binding and activation, as others have reported with EMCV (109).

The induction of some genes by HIV-1 was completely blocked by IFIH1 knockdown, including APOBEC3A and ZBP1 (*SI Appendix*, Tables S1 and S2). In contrast, CXCL10 and ISG15 RNAs were partly induced by HIV-1 in IFIH1 knockdown cells (Fig. 7 *B* and *C* and *SI Appendix*, Tables S1 and S2), conditions under which ISG15 protein was not detected by the flow cytometry assay used in the screen here (Fig. 2*B*). This may indicate that ISG15 protein synthesis requires a high threshold level of ISG15 RNA or that IFIH1 is required to induce other genes that are required for ISG15 protein stability.

Previous experiments in mice indicate that DHX58, the gene that encodes LGP2, potentiates the response of IFIH1 to poly(I:C) or to EMCV (110, 111). EMCV activated human dendritic cells in an IFIH1-dependent manner (Fig. 3*C*), and DHX58 expression was up-regulated by HIV-1 transduction in dendritic cells (*SI Appendix*, Table S1), but DHX58 knockdown did not decrease innate immune activation of human dendritic cells in response to HIV-1 (Fig. 1*C*).

Knockdown of XPO1, the gene encoding the nuclear export protein CRM1, blocked innate immune activation of dendritic

cells by HIV-1 to a comparable extent as did knockdown of IFIH1 or MAVS (Fig. 1*C*). This result confirmed the validity of the loss-of-function screen performed here, in that orthologous experiments reported inhibition with the CRM1-inhibitors leptomycin B and KPT-330, or with a null mutation in HIV-1 *rev* (58, 59). Rev binds to the highly structured RRE present in unspliced and singly spliced HIV-1 transcripts, and possesses a leucine-rich peptide that binds to XPO1, interactions that are both required for nuclear export of the spliced and singly spliced HIV-1 RNAs (112–115). Since unspliced HIV-1 RNA matures dendritic cells in an IFIH1-dependent manner, and requires Rev, the RRE, and XPO1 for nuclear export, and since IFIH1 localizes to the cytoplasm (116), it makes sense that all these factors are required for dendritic cell activation by HIV-1. That being said, cytoplasmic localization of unspliced HIV-1 RNA is not sufficient: HIV-1 bearing disruptive mutations in *rev* and RRE does not activate innate immune signaling, even when nuclear export and p24 translation were fully rescued by heterologous NXF1-dependent nuclear export elements (58, 117). Additionally, the RRE is not sufficient to activate signaling since singly spliced HIV-1 RNA that retains the RRE did not associate with IFIH1 in dendritic cells (Fig. 8, D1A4). Taken together these findings suggest that innate immune detection of HIV-1 requires either HIV-1 sequences within the *gag-pol* intron between D1 and A4, or XPO1-dependent trafficking to a particular subcellular location.

While the data presented here were obtained in dendritic cells and in macrophages, previous studies with the same experimental tools and protocols demonstrated innate immune activation in response to intron-containing HIV-1 RNA in primary CD4+ T cells (58). The latter studies tracked upregulation of HLA-DR and the interferon-stimulated genes MX1 and IFIT1. Additionally, while transduction levels here were boosted by pseudotyping with VSV G, in the presence of Vpx, previous studies showed that innate immune activation occurred after spreading infection with wild-type HIV-1 in the absence of Vpx (58). Importantly, type 1 interferon is elevated in the plasma of people living with HIV-1 (118). Nonetheless, for technical reasons, the genetic perturbation experiments in primary dendritic cells performed here were in the presence of SIV Vpx. Though all experiments were controlled for potential effects of Vpx, the latter protein has been variously reported to inhibit, and in some cases increase the activity of innate immune signaling pathways (119–122).

Taken together, the results here suggest that the chronic inflammation observed In people living with HIV-1 on ART may be caused by IFIH1-dependent activation of innate immune signaling in response to unspliced RNA from HIV-1 proviruses in CD4+ T cells and macrophages. This hypothesis is further supported by correlations between the quantity of cell-associated HIV-1 RNA and plasma levels of inflammatory markers (41, 42), and suggests that drugs which inhibit HIV-1 transcription (123) may decrease inflammation and cardiovascular disease risk in people living with HIV-1.

Materials and Methods

Plasmids. Plasmids used in this study are listed with their corresponding Addgene accession numbers in *SI Appendix*, Table S3. The plasmids themselves, along with their complete nucleotide sequences, are available at https://www.addgene.org/Jeremy_Luban/.

Human Blood. Leukopaks were obtained from anonymous, healthy blood donors (New York Biologics). These experiments were reviewed by the University of Massachusetts Medical School Institutional Review Board and determined to be nonhuman subjects research, as per NIH guidelines, (http://grants.nih.gov/grants/policy/hs/faqs_aps_definitions.htm).

Cell Culture. All cells were cultured in humidified, 5% CO_2 incubators at 37 °C, and monitored for *Mycoplasma* contamination using the *Mycoplasma* Detection kit (Lonza LT07-318). HEK293 cells (ATCC CRL-1573) were used for virus production and were cultured in Dulbecco's Modified Eagle's Medium supplemented with 10% heat-inactivated fetal bovine serum (FBS), 20 mM GlutaMAX (ThermoFisher), 1 mM sodium pyruvate (ThermoFisher), 25 mM HEPES pH 7.2 (Sigma-Aldrich), and 1× MEM nonessential amino acids (ThermoFisher). PBMCs were isolated from leukopaks by gradient centrifugation on Lymphoprep (Axis-Shield Poc AS, catalog no. AXS-1114546). To generate dendritic cells or macrophages, $CD14^+$ mononuclear cells were enriched by positive selection using anti-CD14 antibody microbeads (Miltenyi, catalog no. 130-050-201). Enriched $CD14^+$ cells were plated in RPMI-1640, supplemented with 5% heat-inactivated human AB^+ serum (Omega Scientific), 20 mM GlutaMAX, 1 mM sodium pyruvate, 1× MEM nonessential amino acids and 25 mM HEPES pH 7.2 (RPMI−HS complete), at a density of 2×10^6 cells/mL for dendritic cells or 10^6 cells/mL for macrophages. To differentiate $CD14^+$ cells into dendritic cells, 1:100 human granulocyte-macrophage colony-stimulating factor (hGM-CSF) and 1:100 human interleukin-4 (hIL-4)-conditioned medium was added. To differentiate $CD14^+$ cells into macrophages, 1:100 hGM-CSF-conditioned medium was added. hGM-CSF and hIL-4 were produced from HEK293 cells stably transduced with pAIP-hGM-CSF-co (Addgene no. 74168) or pAIP-hIL-4-co (Addgene no. 74169), as previously described (58).

HIV-1 Vector Production. Twenty-four hours before transfection, 6×10^5 HEK-293E cells were plated per well in six-well plates. A total of 2.49 μg plasmid DNA with 6.25 μL TransIT LT1 transfection reagent (Mirus) in 250 μL Opti-MEM (Gibco) was used in all transfections. For two-part, single-cycle vector, 2.18 μg of pUC57mini NL4-3-env-eGFP (NIH AIDS Reagent Program Cat #13906) was cotransfected with 0.31 μg pMD2.G VSV-G plasmid. Three-part, single-cycle vectors were produced by cotransfecting 1.25 μg minimal lentivector genome plasmid, 0.93 μg *gag-pol* expression plasmid (psPAX2), and 0.31 μg pMD2.G VSV G plasmid. Vpx-containing SIV-VLPs were produced by transfection of 2.18 μg pSIV3+ and 0.31 μg pMD2.G plasmids. Sixteen hours posttransfection, the culture media was changed to the media specific for the cells to be transduced. Viral supernatant was harvested at 72 h, filtered through a 0.45 μm filter, and stored at −80 °C.

Exogenous Reverse Transcriptase Assay. Virions in the transfection supernatant were quantified by a PCR-based assay for reverse transcriptase activity (124). First, 5 μL transfection supernatant was lysed in 5 μL 0.25% Triton X-100, 50 mM KCl, 100 mM Tris-HCl pH 7.4, and 0.4 U/μL RNase inhibitor (RiboLock, ThermoFisher). Viral lysate was then diluted 1:100 in a buffer of 5 mM $(NH_4)_2SO_4$, 20 mM KCl, and 20 mM Tris-HCl pH 8.3. Then, 10 μL was then added to a single-step, RT PCR assay with 35 nM MS2 RNA (IDT) as template, 500 nM of each primer (5′-TCCTGCTCAACTTCCTGTCGAG-3′ and 5′-CACAGGTCAAACCTCCTAGGAATG-3′), and hot-start Taq (Promega) in a buffer of 20 mM Tris-Cl pH 8.3, 5 mM $(NH_4)_2SO_4$, 20 mM KCl, 5 mM $MgCl_2$, 0.1 mg/mL BSA, 1/20,000 SYBR Green I (Invitrogen), and 200 μM dNTPs. The RTPCR was carried out in a BioRad CFX96 real time PCR detection system with the following parameters: 42 °C 20 min, 95 °C 2 min, and 40 cycles (95 °C for 5 s, 60 °C 5 s, 72 °C for 15 s and acquisition at 80 °C for 5 s). Two-part vector transfections (two plasmids) typically yielded 10^7 RT units/μL, and three-part vector transfections (three plasmids) yielded 10^6 RT units/μL.

Transduction. For dendritic cells, 2×10^6 $CD14^+$ monocytes/mL were transduced with 1:4 volume of SIV-VLPs and 1:4 volume of knockdown lentivector, in RPMI. For macrophages, 10^6 $CD14^+$ monocytes/mL were transduced with 1:6 volume of SIV-VLPs and 1:6 volume of knockdown lentivector. The Vpx-containing SIV-VLPs were added to these cultures 30 min prior to addition of the knockdown vector to overcome a SAMHD1 block to lentiviral transduction (125, 126). Transduced cells were selected with 3 μg/mL puromycin (InvivoGen, San Diego, CA, catalog #ant-pr-1) for 3 d, starting 3 d posttransduction.

Infectivity Assay Using Single-Cycle Viruses. For dendritic cells, 2.5×10^5 cells were seeded per well, in a 48-well plate, on the day of virus challenge. Media containing VSV G-pseudotyped lentiviral vector expressing GFP (HIV-1-GFP) was added to challenge cells in a total volume of 250 μL. For macrophages, 2.5×10^5 cells were seeded per well in a 24-well plate and challenged with HIV-1-GFP in a total volume of 500 μL. Additionally, 1:50 volume of SIV-VLPs was added to the

medium during virus challenge of dendritic cells or macrophages. For both cell types, 10^8 RT units/mL of viral vector was used to challenge cells. At 72 h postchallenge, cells were harvested for flow cytometry by scraping. Cells were pelleted at $500 \times g$ for 5 min and fixed in a 1:4 dilution of BD Cytofix Fixation Buffer with phosphate-buffered saline (PBS) without Ca^{2+} and Mg^{2+}, supplemented with 2% FBS and 0.1% NaN_3.

Non-HIV-1 Virus Challenges. SeV Cantell Strain was purchased from Charles River Laboratories. Infections were performed with 200 HA units/mL on dendritic cells and macrophages for 72 h before assay by flow cytometry. EMCV was purchased from ATCC (VR-129B). Infections were performed with MOI 0.1 on dendritic cells and macrophages for 48 h before assay by flow cytometry.

Flow Cytometry. A total of 10^5 cells were pelleted at $500 \times g$ for 5 min and fixed in 100 μL BD Biosciences Cytofix/Cytoperm solution (catalog #554714) for 20 min at 4 °C. Cells were washed twice in 250 μL 1× BD Biosciences Perm/Wash buffer. Human ISG15 APC-conjugated antibody (R&D Sytems, IC8044A) was used at a dilution of 1:100 for intracellular staining. Data were collected on an Accuri C6 (BD Biosciences, San Jose, CA) and plotted with FlowJo software.

Western Blot. Cells were lysed in Hypotonic Lysis Buffer: 20 mM Tris-HCl, pH 7.5, 150 mM NaCl, 10 mM EDTA, 0.5% NP-40, 0.1% Triton X-100, and complete mini protease inhibitor (Sigma-Aldrich) for 20 min on ice. The lysates were mixed 1:1 with 2× Laemmli buffer containing 1:20-diluted 2-mercaptoethanol, boiled for 10 min, and centrifuged at $16,000 \times g$ for 5 min at 4 °C. Samples were run on 4 to 20% SDS-PAGE and transferred to nitrocellulose membranes. Membrane blocking and antibody binding were carried out in TBS Odyssey Blocking Buffer (Li-Cor, Lincoln, NE). Primary antibodies used were rabbit anti-IFIH1/MDA5 (1:1,000 dilution; Proteintech, #21775-1-AP), rabbit anti-DDX58/RIG-I (1:1,000 dilution; Cell Signaling Technology, #3743S), rabbit anti-MAVS (1:1,000 dilution; Thermo Fisher, #PA-5-17256), and mouse anti-β-actin (1:1,000 dilution; Abcam, #ab3280). Goat anti-mouse-680 (Li-Cor, catalog #925-68070) and goat anti-rabbit-800 (Li-Cor, catalog #925-32211) as secondary antibodies were used at 1:10,000 dilutions. Blots were scanned on the Li-Cor Odyssey CLx.

RNA Extraction and RNA-Seq. Total RNA was isolated from 10^6 dendritic cells using the RNeasy Plus Mini kit (Qiagen) with Turbo DNase (ThermoFisher) treatment between washes. For standard poly(A) RNA-Seq, 500 ng RNA from each sample was submitted to Genewiz.

RNA-Seq Processing and Analysis. Quantification of human gene expression was performed on the DolphinNext platform (127) using RSEM (v1.3.1) software's rsem-calculate-expression command, utilizing Star aligner (v2.6.1) and human genome version hg38 (Gencode v34 transcript set). A hybrid genome which included the HIV-1-GFP vector (pUC57mini_NLBN_dEnv_GFP) sequence as well as hg38 was used for viral gene quantification. Alignment (bam) files were converted to tdf format using Igvtools (v2.5.3) and visualized using IGV (v 2.10.0). DESeq2 (v1.30.1) was used for differential gene expression analysis. Donor IDs were included in the design formula ("~ donor + condition") to account for the differences between individuals. DESeq2's rlog variance stabilization transformation was applied to the gene counts, and the donor effect was removed using limma (v3.46.0) software removeBatchEffect function prior to generating the heatmap and PCA plots.

Gene Ontology Analysis. Reactome pathway analysis was performed on https://reactome.org/ based on the 276 highest differentially expressed genes, based on Log2-fold change, comparing HIV-1 transduced Luc-knockdown cells in comparison to HIV-1 transduced IFIH1-knockdown cells. Gene Ontology-produced *P* values (as determined by Fisher's exact test) with FDR correction (Benjamini–Hochberg method) are shown.

f-CLIP. Protein A-coated magnetic Dynabeads (Thermo, 10001D) were washed 3 times with CLIP buffer, PBS (pH 7.4), 0.1% (w/v) SDS, 0.5% (w/v) deoxycholate, 0.5% (v/v) NP-40, protease inhibitor (Pierce, A32955), and RNAse inhibitor (Thermo, EO0382) and incubated with anti-MDA5 (IFIH1) antibody (Proteintech, 21775-1-AP) or anti-RIG-I (DDX58) antibody (Proteintech, 25068-1-AP) for 1 h at 4 °C. Dendritic cells were seeded at 10^6 per mL in RPMI-HS complete, with Vpx+ SIV-VLP transfection supernatant added at a dilution of 1:4. After 1 h, the cells were incubated with 1:4 volume of VSV G-pseudotyped, pUC57mini

NL4-3-env-eGFP (NIH AIDS Reagent Program Cat #13906). Seventy-two hours posttransduction, cells were harvested and washed with ice-cold PBS. Cells were cross-linked with freshly prepared 0.1% formaldehyde for 10 min at room temperature and quenched by adding 1.5 M glycine in PBS to a final concentration of 150 mM and incubating for 10 min at room temperature with gentle shaking. Cross-linked cells were washed with PBS, resuspended in CLIP buffer, and sonicated with the Diagenode Bioruptor (10 cycles of 30 s On, 30 s Off, at 4 °C). The lysate was centrifuged at 10,000 × g for 10 min at 4 °C. The supernatant was mixed with the antibody-coated Dynabeads, incubated on a rotator overnight at 4 °C. The flowthrough was collected for western blot analysis to check for depletion of the protein of interest. The beads were washed three times with CLIP buffer. Then, 10 μL of the resuspended beads in CLIP buffer was collected for western blot analysis to check the recovery of the protein of interest. The washed beads were incubated in proteinase K buffer [400 mM Tris-HCl (pH 7.4), 200 mM NaCl, 40 mM EDTA, and 4% (w/v) SDS] with 10 μL of proteinase K (Thermo, EO0491) for 1 h at 65 °C with gentle agitation. Then, 500 μL RNAzol was added to the supernatant, and RNA was isolated by isopropanol precipitation. The precipitated RNA was washed with 75% ethanol, air dried, and resuspended in 20 μL nuclease-free water. RNA was treated with DNAse I (Invitrogen, AM1907). Equal amounts of input RNA, as measured by NanoDrop 2000 (Thermo), were used to make cDNA with iScript Advanced cDNA Synthesis Kit (BioRad, 1725037). cDNA was amplified by qPCR with iTaq

Universal SYBR Green Supermix (BioRad, 1725121), using HIV-1-specific primers (gag, pol RT, pol IN, D1A4, and D4A7) or primers targeting the cellular gene ACTB (primer sequences in *SI Appendix*, Table S4), with a BioRad CFX96 Real Time PCR head on a C1000 Touch Thermocycler, with the following settings: 95 °C for 30 s, then (95 °C for 10 s, 60 °C for 30 s) × 40 cycles, followed by a melt curve from 65 to 95 °C with increments of 0.5 °C.

Statistical Analysis. Experimental n values and information regarding specific statistical tests can be found in the figure legends. All statistical analyses were performed using PRISM 8.2 software (GraphPad Software, La Jolla, CA).

Data, Materials, and Software Availability. The data that support the findings of this study are available within the manuscript and in *SI Appendix*, Tables S1 and S2. RNA-Seq datasets generated here can be found at the NCBI Gene Expression Omnibus (GEO): GSE201250 (128). The plasmids described in *SI Appendix*, Table S3, along with their complete nucleotide sequences, are available at https://www.addgene.org/Jeremy_Luban/ (129).

1. J. K. Wong *et al.*, Recovery of replication-competent HIV despite prolonged suppression of plasma viremia. *Science* **278**, 1291–1295 (1997).
2. N. F. McMyn *et al.*, The latent reservoir of inducible, infectious HIV-1 does not decrease despite decades of antiretroviral therapy. *J. Clin. Invest.* **133**, e171554 (2023).
3. P. W. Hunt *et al.*, T cell activation is associated with lower CD4+ T cell gains in human immunodeficiency virus-infected patients with sustained viral suppression during antiretroviral therapy. *J. Infect. Dis.* **187**, 1534–1543 (2003).
4. J. Z. Li *et al.*, Antiretroviral therapy reduces T-cell activation and immune exhaustion markers in human immunodeficiency virus controllers. *Clin. Infect. Dis.* **70**, 1636–1642 (2020).
5. D. C. Douek, M. Roederer, R. A. Koup, Emerging concepts in the immunopathogenesis of AIDS. *Annu. Rev. Med.* **60**, 471–484 (2009).
6. S. G. Deeks, R. Tracy, D. C. Douek, Systemic effects of inflammation on health during chronic HIV infection. *Immunity* **39**, 633–645 (2013).
7. N. I. Wada *et al.*, The effect of HAART-induced HIV suppression on circulating markers of inflammation and immune activation. *AIDS* **29**, 463–471 (2015).
8. E. Kosmider *et al.*, Observational study of effects of HIV acquisition and antiretroviral treatment on biomarkers of systemic immune activation. medRxiv [Preprint] (2023). https://doi.org/10.1101/2023.07.07.23292352 (Accessed 28 June 2024).
9. M. Nasi *et al.*, Aging with HIV infection: A journey to the center of inflammAIDS, immunosenescence and neuroHIV. *Immunol. Lett.* **162**, 329–333 (2014).
10. M. S. Freiberg *et al.*, HIV infection and the risk of acute myocardial infarction. *JAMA Intern. Med.* **173**, 614–622 (2013).
11. R. A. McKibben *et al.*, Elevated levels of monocyte activation markers are associated with subclinical atherosclerosis in men with and those without HIV infection. *J. Infect. Dis.* **211**, 1219–1228 (2015).
12. A. Sinha *et al.*, Role of T-cell dysfunction, inflammation, and coagulation in microvascular disease in HIV. *J. Am. Heart Assoc.* **5**, e004243 (2016).
13. V. C. Marconi *et al.*, Randomized trial of ruxolitinib in antiretroviral-treated adults with human immunodeficiency virus. *Clin. Infect. Dis.* **74**, 95–104 (2022).
14. S. K. Grinspoon *et al.*, Pitavastatin to prevent cardiovascular disease in HIV infection. *N. Engl. J. Med.* **389**, 687–699 (2023).
15. M. Smit *et al.*, Future challenges for clinical care of an ageing population infected with HIV: A modelling study. *Lancet Infect. Dis.* **15**, 810–818 (2015).
16. S. Krishnan *et al.*, Metabolic syndrome before and after initiation of antiretroviral therapy in treatment-naive HIV-infected individuals. *J. Acquir. Immune Defic. Syndr.* **61**, 381–389 (2012).
17. W. D. F. Venter *et al.*, Dolutegravir plus two different prodrugs of tenofovir to treat HIV. *N. Engl. J. Med.* **381**, 803–815 (2019).
18. NAMSAL ANRS 12313 Study Group *et al.*, Dolutegravir-based or low-dose efavirenz-based regimen for the treatment of HIV-1. *N. Engl. J. Med.* **381**, 816–826 (2019).
19. P. Y. Hsue *et al.*, Increased carotid intima-media thickness in HIV patients is associated with increased cytomegalovirus-specific T-cell responses. *AIDS* **20**, 2275–2283 (2006).
20. R. C. Hechter *et al.*, Herpes simplex virus type 2 (HSV-2) as a coronary atherosclerosis risk factor in HIV-infected men: Multicenter AIDS cohort study. *Atherosclerosis* **223**, 433–436 (2012).
21. M. M. Sajadi, R. Pulijala, R. R. Redfield, R. Talwani, Chronic immune activation and decreased CD4 cell counts associated with hepatitis C infection in HIV-1 natural viral suppressors. *AIDS* **26**, 1879–1884 (2012).
22. S. Gianella *et al.*, Cytomegalovirus replication in semen is associated with higher levels of proviral HIV DNA and CD4+ T cell activation during antiretroviral treatment. *J. Virol.* **88**, 7818–7827 (2014).
23. J. M. Brenchley *et al.*, Microbial translocation is a cause of systemic immune activation in chronic HIV infection. *Nat. Med.* **12**, 1365–1371 (2006).
24. A. R. Stacey *et al.*, Induction of a striking systemic cytokine cascade prior to peak viremia in acute human immunodeficiency virus type 1 infection, in contrast to more modest and delayed responses in acute hepatitis B and C virus infections. *J. Virol.* **83**, 3719–3733 (2009).
25. H. N. Kløverpris *et al.*, Innate lymphoid cells are depleted irreversibly during acute HIV-1 infection in the absence of viral suppression. *Immunity* **44**, 391–405 (2016).
26. Y. Wang *et al.*, HIV-1-induced cytokines deplete homeostatic innate lymphoid cells and expand TCF7-dependent memory NK cells. *Nat. Immunol.* **21**, 274–286 (2020).
27. D. Finzi *et al.*, Identification of a reservoir for HIV-1 in patients on highly active antiretroviral therapy. *Science* **278**, 1295–1300 (1997).
28. T. W. Chun *et al.*, Presence of an inducible HIV-1 latent reservoir during highly active antiretroviral therapy. *Proc. Natl. Acad. Sci. U.S.A.* **94**, 13193–13197 (1997).
29. A. J. Kandathil, S. Sugawara, A. Balagopal, Are T cells the only HIV-1 reservoir? *Retrovirology* **13**, 86 (2016).
30. A. J. Kandathil *et al.*, No recovery of replication-competent HIV-1 from human liver macrophages. *J. Clin. Invest.* **128**, 4501–4509 (2018).
31. J. H. Campbell, A. C. Hearps, G. E. Martin, K. C. Williams, S. M. Crowe, The importance of monocytes and macrophages in HIV pathogenesis, treatment, and cure. *AIDS* **28**, 2175–2187 (2014).
32. J. B. Honeycutt *et al.*, HIV persistence in tissue macrophages of humanized myeloid-only mice during antiretroviral therapy. *Nat. Med.* **23**, 638–643 (2017).
33. M. Araínga *et al.*, A mature macrophage is a principal HIV-1 cellular reservoir in humanized mice after treatment with long acting antiretroviral therapy. *Retrovirology* **14**, 17 (2017).
34. R. T. Veenhuis *et al.*, Monocyte-derived macrophages contain persistent latent HIV reservoirs. *Nat. Microbiol.* **8**, 833–844 (2023).
35. Y.-C. Ho *et al.*, Replication-competent noninduced proviruses in the latent reservoir increase barrier to HIV-1 cure. *Cell* **155**, 540–551 (2013).
36. K. M. Bruner *et al.*, Defective proviruses rapidly accumulate during acute HIV-1 infection. *Nat. Med.* **22**, 1043–1049 (2016).
37. K. M. Bruner *et al.*, A quantitative approach for measuring the reservoir of latent HIV-1 proviruses. *Nature* **566**, 120–125 (2019), 10.1038/s41586-019-0898-8.
38. A. Wiegand *et al.*, Single-cell analysis of HIV-1 transcriptional activity reveals expression of proviruses in expanded clones during ART. *Proc. Natl. Acad. Sci. U.S.A.* **114**, E3659–E3668 (2017).
39. H. Imamichi *et al.*, Defective HIV-1 proviruses produce novel protein-coding RNA species in HIV-infected patients on combination antiretroviral therapy. *Proc. Natl. Acad. Sci. U.S.A.* **113**, 8783–8788 (2016).
40. R. A. Pollack *et al.*, Defective HIV-1 proviruses are expressed and can be recognized by cytotoxic T lymphocytes, which shape the proviral landscape. *Cell Host Microbe* **21**, 494–506.e4 (2017).
41. A. Olson, C. Coote, J. E. Snyder-Cappione, N. Lin, M. Sagar, HIV-1 transcription but not intact provirus levels are associated with systemic inflammation. *J. Infect. Dis.* **223**, 1934–1942 (2020), 10.1093/infdis/jiaa657.
42. R. El-Diwany *et al.*, Intracellular HIV-1 RNA and CD4+ T-cell activation in patients starting antiretrovirals. *AIDS* **31**, 1405–1414 (2017).
43. J.-F. Fonteneau *et al.*, Human immunodeficiency virus type 1 activates plasmacytoid dendritic cells and concomitantly induces the bystander maturation of myeloid dendritic cells. *J. Virol.* **78**, 5223–5232 (2004).
44. A.-S. Beignon *et al.*, Endocytosis of HIV-1 activates plasmacytoid dendritic cells via Toll-like receptor–viral RNA interactions. *J. Clin. Invest.* **115**, 3265–3275 (2005).
45. M. O'Brien, O. Manches, N. Bhardwaj, Plasmacytoid dendritic cells in HIV infection. *Adv. Exp. Med. Biol.* **762**, 71–107 (2012), 10.1007/978-1-4614-4433-6_3.
46. M. Dominguez-Villar, A.-S. Gautron, M. de Marcken, M. J. Keller, D. A. Hafler, TLR7 induces anergy in human CD4(+) T cells. *Nat. Immunol.* **16**, 118–128 (2015).
47. D. Jarrossay, G. Napolitani, M. Colonna, F. Sallusto, A. Lanzavecchia, Specialization and complementarity in microbial molecule recognition by human myeloid and plasmacytoid dendritic cells. *Eur. J. Immunol.* **31**, 3388–3393 (2001).
48. A. Izaguirre *et al.*, Comparative analysis of IRF and IFN-alpha expression in human plasmacytoid and monocyte-derived dendritic cells. *J. Leukoc. Biol.* **74**, 1125–1138 (2003).
49. A. Smed-Sörensen *et al.*, Differential susceptibility to human immunodeficiency virus type 1 infection of myeloid and plasmacytoid dendritic cells. *J. Virol.* **79**, 8861–8869 (2005).
50. M. Solis *et al.*, RIG-I-mediated antiviral signaling is inhibited in HIV-1 infection by a protease-mediated sequestration of RIG-I. *J. Virol.* **85**, 1224–1236 (2011).
51. R. K. Berg *et al.*, Genomic HIV RNA induces innate immune responses through RIG-I-dependent sensing of secondary-structured RNA. *PLoS One* **7**, e29291 (2012).
52. D. Gao *et al.*, Cyclic GMP-AMP synthase is an innate immune sensor of HIV and other retroviruses. *Science* **341**, 903–906 (2013).

53. J. S. Johnson *et al.*, Reshaping of the dendritic cell chromatin landscape and interferon pathways during HIV infection. *Cell Host Microbe* **23**, 366–381.e9 (2018).

54. J. Vermeire *et al.*, HIV triggers a cGAS-dependent, Vpu- and Vpr-regulated type I interferon response in CD4+ T cells. *Cell Rep.* **17**, 413–424 (2016), 10.1016/j.celrep.2016.09.023.

55. J. Rasaiyaah *et al.*, HIV-1 evades innate immune recognition through specific cofactor recruitment. *Nature* **503**, 402–405 (2013).

56. X. Lahaye *et al.*, The capsids of HIV-1 and HIV-2 determine immune detection of the viral cDNA by the innate sensor cGAS in dendritic cells. *Immunity* **39**, 1132–1142 (2013).

57. R. K. Berg *et al.*, T cells detect intracellular DNA but fail to induce type I IFN responses: Implications for restriction of HIV replication. *PLoS One* **9**, e84513 (2014), 10.1371/journal.pone.0084513.

58. S. M. McCauley *et al.*, Intron-containing RNA from the HIV-1 provirus activates type I interferon and inflammatory cytokines. *Nat. Commun.* **9**, 5305 (2018).

59. H. Akiyama *et al.*, HIV-1 intron-containing RNA expression induces innate immune activation and T cell dysfunction. *Nat. Commun.* **9**, 3450 (2018).

60. C. Elsner *et al.*, Absence of cGAS-mediated type I IFN responses in HIV-1-infected T cells. *Proc. Natl. Acad. Sci. U.S.A.* **117**, 19475–19486 (2020).

61. M. A. Siddiqui *et al.*, A novel phenotype links HIV-1 capsid stability to cGAS-mediated DNA sensing. *J. Virol.* **93**, e00706-19 (2019).

62. E. Martin-Gayo *et al.*, Cooperation between cGAS and RIG-I sensing pathways enables improved innate recognition of HIV-1 by myeloid dendritic cells in elite controllers. *Front. Immunol.* **13**, 1017164 (2022).

63. L. Zuliani-Alvarez *et al.*, Evasion of cGAS and TRIM5 defines pandemic HIV. *Nat. Microbiol.* **7**, 1762–1776 (2022).

64. G. Papa *et al.*, IP6-stabilised HIV capsids evade cGAS/STING-mediated host immune sensing. *EMBO Rep.* **24**, e56275 (2023).

65. N. Manel *et al.*, A cryptic sensor for HIV-1 activates antiviral innate immunity in dendritic cells. *Nature* **467**, 214–217 (2010).

66. R. A. Knoener, J. T. Becker, M. Scalf, N. M. Sherer, L. M. Smith, Elucidating the in vivo interactome of HIV-1 RNA by hybridization capture and mass spectrometry. *Sci. Rep.* **7**, 16965 (2017).

67. A. Kula *et al.*, Characterization of the HIV-1 RNA associated proteome identifies Matrin 3 as a nuclear cofactor of Rev function. *Retrovirology* **8**, 60 (2011).

68. V. Marchand *et al.*, Identification of protein partners of the human immunodeficiency virus 1 tat/rev exon 3 leads to the discovery of a new HIV-1 splicing regulator, protein hnRNP K. *RNA Biol.* **8**, 325–342 (2011).

69. K. Kim *et al.*, Cyclophilin A protects HIV-1 from restriction by human TRIM5α. *Nat. Microbiol.* **4**, 2044–2051 (2019).

70. C. Goujon *et al.*, With a little help from a friend: Increasing HIV transduction of monocyte-derived dendritic cells with virion-like particles of SIV(MAC). *Gene Ther.* **13**, 991–994 (2006).

71. A. Granelli-Piperno, L. Zhong, P. Haslett, J. Jacobson, R. M. Steinman, Dendritic cells, infected with vesicular stomatitis virus-pseudotyped HIV-1, present viral antigens to CD4+ and CD8+ T cells from HIV-1-infected individuals. *J. Immunol.* **165**, 6620–6626 (2000).

72. P. Nakhaei, P. Genin, A. Civas, J. Hiscott, RIG-I-like receptors: Sensing and responding to RNA virus infection. *Semin. Immunol.* **21**, 215–222 (2009).

73. Y.-M. Loo, M. Gale Jr., Immune signaling by RIG-I-like receptors. *Immunity* **34**, 680–692 (2011).

74. L. Gitlin *et al.*, Essential role of mda-5 in type I IFN responses to polyriboinosinic:Polyribocytidylic acid and encephalomyocarditis picornavirus. *Proc. Natl. Acad. Sci. U.S.A.* **103**, 8459–8464 (2006), 10.1073/pnas.0603082103.

75. H. Kato *et al.*, Cell type-specific involvement of rig-i in antiviral response. *Immunity* **23**, 19–28 (2005), 10.1016/j.immuni.2005.04.010.

76. H. Kato *et al.*, Differential roles of MDA5 and RIG-I helicases in the recognition of RNA viruses. *Nature* **441**, 101–105 (2006), 10.1038/nature04734.

77. J. Andrejeva *et al.*, The V proteins of paramyxoviruses bind the IFN-inducible RNA helicase, mda-5, and inhibit its activation of the IFN-β promoter. *Proc. Natl. Acad. Sci. U.S.A.* **101**, 17264–17269 (2004).

78. K. Childs *et al.*, mda-5, but not RIG-I, is a common target for paramyxovirus V proteins. *Virology* **359**, 190–200 (2007).

79. K. S. Childs, J. Andrejeva, R. E. Randall, S. Goodbourn, Mechanism of mda-5 Inhibition by paramyxovirus V proteins. *J. Virol.* **83**, 1465–1473 (2009).

80. J.-P. Parisien *et al.*, A shared interface mediates paramyxovirus interference with antiviral RNA helicases MDA5 and LGP2. *J. Virol.* **83**, 7252–7260 (2009).

81. C. Motz *et al.*, Paramyxovirus V proteins disrupt the fold of the RNA sensor MDA5 to inhibit antiviral signaling. *Science* **339**, 690–693 (2013).

82. X. Jiang *et al.*, Ubiquitin-induced oligomerization of the RNA sensors RIG-I and MDA5 activates antiviral innate immune response. *Immunity* **36**, 959–973 (2012).

83. B. Wu *et al.*, Structural basis for dsRNA recognition, filament formation, and antiviral signal activation by MDA5. *Cell* **152**, 276–289 (2013).

84. E. Wies *et al.*, Dephosphorylation of the RNA sensors RIG-I and MDA5 by the phosphatase PP1 is essential for innate immune signaling. *Immunity* **38**, 437–449 (2013).

85. A. Peisley *et al.*, Cooperative assembly and dynamic disassembly of MDA5 filaments for viral dsRNA recognition. *Proc. Natl. Acad. Sci. U.S.A.* **108**, 21010–21015 (2011).

86. I. C. Berke, Y. Modis, MDA5 cooperatively forms dimers and ATP-sensitive filaments upon binding double-stranded RNA. *EMBO J.* **31**, 1714–1726 (2012).

87. Q. Yu, Q. Qu, Y. Modis, Cryo-EM structures of MDA5-dsRNA filaments at different stages of ATP hydrolysis. *Mol. Cell* **72**, 999–1012.e6 (2018).

88. B. Kim, V. N. Kim, fCLIP-seq for transcriptomic footprinting of dsRNA-binding proteins: Lessons from DROSHA. *Methods* **152**, 3–11 (2019).

89. E. Meylan *et al.*, Cardif is an adaptor protein in the RIG-I antiviral pathway and is targeted by hepatitis C virus. *Nature* **437**, 1167–1172 (2005).

90. T. Kawai *et al.*, IPS-1, an adaptor triggering RIG-I- and Mda5-mediated type I interferon induction. *Nat. Immunol.* **6**, 981–988 (2005).

91. R. B. Seth, L. Sun, C.-K. Ea, Z. J. Chen, Identification and characterization of MAVS, a mitochondrial antiviral signaling protein that activates NF-κB and IRF3. *Cell* **122**, 669–682 (2005).

92. L.-G. Xu *et al.*, VISA is an adapter protein required for virus-triggered IFN-beta signaling. *Mol. Cell* **19**, 727–740 (2005).

93. M. Llano *et al.*, An essential role for LEDGF/p75 in HIV integration. *Science* **314**, 461–464 (2006).

94. V. Hornung *et al.*, 5′-Triphosphate RNA is the ligand for RIG-I. *Science* **314**, 994–997 (2006).

95. A. Pichlmair *et al.*, RIG-I-mediated antiviral responses to single-stranded RNA bearing 5′-phosphates. *Science* **314**, 997–1001 (2006).

96. A. Schmidt *et al.*, 5′-triphosphate RNA requires base-paired structures to activate antiviral signaling via RIG-I. *Proc. Natl. Acad. Sci. U.S.A.* **106**, 12067–12072 (2009).

97. M. Schlee *et al.*, Recognition of 5′ triphosphate by RIG-I helicase requires short blunt double-stranded RNA as contained in panhandle of negative-strand virus. *Immunity* **31**, 25–34 (2009).

98. J. Rehwinkel *et al.*, RIG-I detects viral genomic RNA during negative-strand RNA virus infection. *Cell* **140**, 397–408 (2010).

99. A. Baum, R. Sachidanandam, A. García-Sastre, Preference of RIG-I for short viral RNA molecules in infected cells revealed by next-generation sequencing. *Proc. Natl. Acad. Sci. U.S.A.* **107**, 16303–16308 (2010).

100. D. Goubau *et al.*, Antiviral immunity via RIG-I-mediated recognition of RNA bearing 5′-diphosphates. *Nature* **514**, 372–375 (2014).

101. C. Schuberth-Wagner *et al.*, A conserved histidine in the RNA sensor RIG-I controls immune tolerance to N1-2′O-methylated self RNA. *Immunity* **43**, 41–51 (2015).

102. Y.-L. Chiu *et al.*, Tat stimulates cotranscriptional capping of HIV mRNA. *Mol. Cell* **10**, 585–597 (2002).

103. V. S. R. K. Yedavalli, K.-T. Jeang, Trimethylguanosine capping selectively promotes expression of Rev-dependent HIV-1 RNAs. *Proc. Natl. Acad. Sci. U.S.A.* **107**, 14787–14792 (2010).

104. H. Kato *et al.*, Length-dependent recognition of double-stranded ribonucleic acids by retinoic acid–inducible gene-I and melanoma differentiation–associated gene 5. *J. Exp. Med.* **205**, 1601–1610 (2008).

105. Q. Feng *et al.*, MDA5 detects the double-stranded RNA replicative form in picornavirus-infected cells. *Cell Rep.* **2**, 1187–1196 (2012).

106. K. Triantafilou *et al.*, Visualisation of direct interaction of MDA5 and the dsRNA replicative intermediate form of positive strand RNA viruses. *J. Cell Sci.* **125**, 4761–4769 (2012), 10.1242/jcs.103887.

107. J. M. Watts *et al.*, Architecture and secondary structure of an entire HIV-1 RNA genome. *Nature* **460**, 711–716 (2009).

108. P. J. Tomezsko *et al.*, Determination of RNA structural diversity and its role in HIV-1 RNA splicing. *Nature* **582**, 438–442 (2020).

109. A. Pichlmair *et al.*, Activation of MDA5 requires higher-order RNA structures generated during virus infection. *J. Virol.* **83**, 10761–10769 (2009).

110. S. Deddouche *et al.*, Identification of an LGP2-associated MDA5 agonist in picornavirus-infected cells. *Elife* **3**, e01535 (2014).

111. K. S. Childs, R. E. Randall, S. Goodbourn, LGP2 plays a critical role in sensitizing mda-5 to activation by double-stranded RNA. *PLoS One* **8**, e64202 (2013).

112. C. A. Rosen, E. Terwilliger, A. Dayton, J. G. Sodroski, W. A. Haseltine, Intragenic cis-acting art gene-responsive sequences of the human immunodeficiency virus. *Proc. Natl. Acad. Sci. U.S.A.* **85**, 2071–2075 (1988).

113. M. H. Malim, J. Hauber, S. Y. Le, J. V. Maizel, B. R. Cullen, The HIV-1 rev trans-activator acts through a structured target sequence to activate nuclear export of unspliced viral mRNA. *Nature* **338**, 254–257 (1989).

114. B. R. Cullen, M. H. Malim, The HIV-1 Rev protein: Prototype of a novel class of eukaryotic post-transcriptional regulators. *Trends Biochem. Sci.* **16**, 346–350 (1991).

115. M. Fornerod, M. Ohno, M. Yoshida, I. W. Mattaj, CRM1 is an export receptor for leucine-rich nuclear export signals. *Cell* **90**, 1051–1060 (1997).

116. D.-C. Kang *et al.*, mda-5: An interferon-inducible putative RNA helicase with double-stranded RNA-dependent ATPase activity and melanoma growth-suppressive properties. *Proc. Natl. Acad. Sci. U.S.A.* **99**, 637–642 (2002).

117. S. Smulevitch *et al.*, RTE and CTE mRNA export elements synergistically increase expression of unstable, Rev-dependent HIV and SIV mRNAs. *Retrovirology* **3**, 1–9 (2006).

118. G. A. D. Hardy *et al.*, Interferon-α is the primary plasma type-I IFN in HIV-1 infection and correlates with immune activation and disease markers. *PLoS One* **8**, e56527 (2013).

119. X. Cheng, L. Ratner, HIV-2 Vpx protein interacts with interferon regulatory factor 5 (IRF5) and inhibits its function. *J. Biol. Chem.* **289**, 9146–9157 (2014).

120. J. Su *et al.*, HIV-2/SIV Vpx targets a novel functional domain of STING to selectively inhibit cGAS-STING-mediated NF-κB signalling. *Nat. Microbiol.* **4**, 2552–2564 (2019).

121. O. Cingöz, N. D. Arnow, M. Puig Torrents, N. Bannert, Vpx enhances innate immune responses independently of SAMHD1 during HIV-1 infection. *Retrovirology* **18**, 4 (2021).

122. D. L. Fink *et al.*, HIV-2/SIV Vpx antagonises NF-κB activation by targeting p65. *Retrovirology* **19**, 2 (2022).

123. C. Li, L. Mori, S. T. Valente, The block-and-lock strategy for human immunodeficiency virus cure: Lessons learned from didehydro-cortistatin A. *J. Infect. Dis.* **223**, 46–53 (2021).

124. T. Pertel *et al.*, TRIM5 is an innate immune sensor for the retrovirus capsid lattice. *Nature* **472**, 361–365 (2011).

125. N. Laguette *et al.*, SAMHD1 is the dendritic- and myeloid-cell-specific HIV-1 restriction factor counteracted by Vpx. *Nature* **474**, 654–657 (2011).

126. K. Hrecka *et al.*, Vpx relieves inhibition of HIV-1 infection of macrophages mediated by the SAMHD1 protein. *Nature* **474**, 658–661 (2011).

127. O. Yukselen, O. Turkyilmaz, A. R. Ozturk, M. Garber, A. Kucukural, DolphinNext: A distributed data processing platform for high throughput genomics. *BMC Genomics* **21**, 310 (2020).

128. H. M. Guney, O. Aydemir, J. Luban, Analysis of monocyte-derived dendritic cell transcriptome upon HIV-1 challenge and effect of MDA5 knockdown. Gene Expression Omnibus. https://www.ncbi.nlm.nih.gov/geo/query/acc.cgi?acc=GSE201250. Deposited 14 December 2023.

129. J. Luban, Luban Lab Plasmids. Addgene plasmid repository. https://www.addgene.org/Jeremy_Luban/. Deposited 28 June 2024.